

Trends in Atomic Adsorption on Titanium Carbide and Nitride

Aleksandra Vojvodic,* Carlo Ruberto, and Bengt I. Lundqvist

Department of Applied Physics, Chalmers University of Technology, SE-412 96 Göteborg, Sweden

Extensive density-functional calculations on atomic chemisorption of H, B, C, N, O, F, Al, Si, P, S, and Cl on the polar TiC(111) and TiN(111) yield similar adsorption trends for the two surfaces: (i) pyramid-like adsorption-energy trends along the adatom periods; (ii) strongest adsorption for O, C, N, S, and F; (iii) large adsorption variety; (iv) record-high adsorption energy for O (8.4 – 8.8 eV). However, a stronger adsorption on TiN is found for elements on the left of the periodic table and on TiC for elements on the right. The results support that a concerted-coupling model, proposed for chemisorption on TiC, applies also to TiN.

Keywords: Density-functional calculations, Titanium carbide, Titanium nitride, Adatoms, Adsorption, Chemisorption, Surface energy, Growth.

I. INTRODUCTION

Titanium carbonitrides, Ti(C,N), are in broad technical use, including mechanical applications such as wear-resistant cutting-tool coatings, and electronic ones, such as TiC as substrate for growth of SiC, graphene, and other carbidic nanostructures, and TiN as diffusion barrier in integrated circuits. Also, the bonding nature of the technologically fascinating MAX phases, like Ti₃SiC₂ and Ti₃AlC₂, relates to the bonding between “sheets” of Ti₆C octahedra and Al/Si atoms [1]. Common to processes like these is an initial chemisorption step that calls for a fundamental understanding of atomic chemisorption on these materials. Their intriguing combination of covalency, ionicity, and metallicity puts TiC and TiN into a class of their own, suggesting unique chemisorption properties. Can these be described with models used for transition-metal substrates? How do the activity and other chemisorption properties vary when going from TiC to TiN or when changing the relative amounts of C and N in Ti(C,N)? The higher chemical activity of the TiC(111) surface, compared to TiC(001), has been suggested to be due to the presence of a surface state (SS) on TiC(111) [2]. Studies of SS’s on TiN(111) and of their importance for reactivity still seem to be lacking in the literature.

In a separate study, we perform an extensive trend study of atomic chemisorption on the TiC(111) surface, there providing a model for the description of chemisorption [3]. Here, we extend our study to TiN(111): how do TiC(111) and TiN(111) compare concerning atomic adsorption? In particular, how does the change of substrate influence adsorption strength, adsorption-energy trends, adsorption-site preference, adsorption geometry, and diffusion barriers? What are the implications of such results for the nature of the chemisorption on TiC and TiN and for their technological applications?

II. COMPUTATIONAL METHOD

First-principles calculations based on the density-functional theory (DFT) are performed with the pseudopotential-plane-wave-based code **dacapo**, with the PW91 generalized-gradient approximation [4]. Slabs with 4 TiX (X = C or N) bilayers (one bilayer corresponds to one Ti and one X atomic layer) are used. Each atomic layer in TiC (TiN) is composed of 6 (9) atoms. Convergence is tested by increasing the number of atoms per layer, the **k**-point sampling, the plane-wave cutoff, the number of layers, and the vacuum thickness. The adatom and the top three TiX bilayers are allowed to relax in all directions until forces are less than 0.05 eV/Å. Charge localization around individual atoms is measured with the “atoms-in-molecule” method of Bader [5]. The adsorption energies E_{ads} are calculated as $E_{\text{ads}} = |E_{\text{slab+adatom}} - E_{\text{clean slab}} - E_{\text{free adatom}}|$.

III. BRIEF ACCOUNT OF TiC RESULTS

The stable bulk crystal structure of TiC is the rock-salt structure, with lattice constant of 4.332 Å from our structure optimization [3] (experiment: 4.330 Å [6]) and a calculated cohesive energy of 14.75 eV. The bonding [3, 8] is characterized by spatially directed Ti–C bonds that secure strength, structure, and hardness [7]. Covalency is manifested by the strong splitting of the electron states into an empty conduction band (CB) of antibonding C2*p*–Ti3*d* states above the Fermi level E_F , and an occupied upper valence band (UVB) of bonding C2*p*–Ti3*d* states, extending between –6.1 eV (all energies are given relative to E_F) and E_F . The Fermi level lies in the pseudogap between the CB and the UVB, where the low but nonvanishing DOS gives the metallic character. A considerable ionic contribution to the bonds is inferred from the dominance of Ti-localized states in the CB and of C-localized states in the UVB, as well as from the charge transfer from Ti to C (1.51 electrons from our Bader analysis). Our state-resolved analyses of the UVB show also a dominance of direct C–C bonding states in the low-energy DOS peak of the UVB [3]. A lower va-

*Electronic address: alevoj@fy.chalmers.se

lence band (LVB), consisting of non-bonding $C2s$ states, extends between -12.8 and -8.4 eV.

The polar $TiC(111)$ surface is Ti terminated, chemically very active, and has a strong SS near the Fermi energy E_F [2]. This SS consists of strongly localized surface-Ti $3d$ electrons that extend out into the vacuum and to neighboring surface fcc sites, where they connect with the electron clouds from the neighboring surface Ti atoms, avoiding the regions corresponding to the hcp adsorption sites. In contrast, the more stable $TiC(001)$ surface is much less active and lacks a major SS [2]. Like bulk TiC, the $TiC(111)$ surface has a UVB, dominated by $C2p$ states in covalent Ti-C bonds and, in the lower UVB region, C-C bonds, and a separated LVB of $C2s$ states.

Our calculations [3] show TiC able to produce atomic chemisorption energies in a wide range, with great sensitivity to adsorbate species [between the record-high 8.8 eV for O and the low 3.4 eV for Al in the most stable site (fcc) on $TiC(111)$], as well as to substrate face [5.0 eV for O in the on-top-C $TiC(001)$ site] and adsorption site [*e.g.*, 7.9 and 6.5 eV for hcp and top O, respectively, on $TiC(111)$].

On $TiC(111)$, our calculated adsorption energies E_{ads} for the second- and third-period elements B, C, N, O, F, Al, Si, P, S, and Cl in fcc, hcp, and top sites [3] show pyramid-shaped trends along each period, with strongest binding for the group-VI elements (O and S) (see Fig. 3 for the fcc energies, similar trends are obtained for hcp and top). The adsorption strength weakens monotonically when moving away from group VI in each period and when moving from period 2 to period 3. The exception is for C and N, whose E_{ads} values lie very close. For all adatoms, the relative site stability is $fcc > hcp > top$. The bridge site is unstable for all adatoms and relaxes to the fcc site.

Detailed analyses and comparisons of the calculated DOS's for the different adatoms yield a model for the chemisorption mechanism that is based on the Newns-Anderson (NA) model [9]. In this concerted-coupling model [3], two different types of adatom-substrate couplings work together in a concerted way: (i) the adatom frontier orbitals overlap strongly with the Fermi-level SS that sticks out from the surface, thus giving a strong chemisorption in the NA sense, with well separated bonding (just below the adatom level, deeper for more electronegative adatoms) and antibonding levels (just above the SS and the Fermi level); (ii) in addition, for several adatoms, there is a chemisorptive interaction with substrate states in the UVB, with varying strength through the adatom period, as the SS-modified adlevel traces different parts of the varying TiC UVB features.

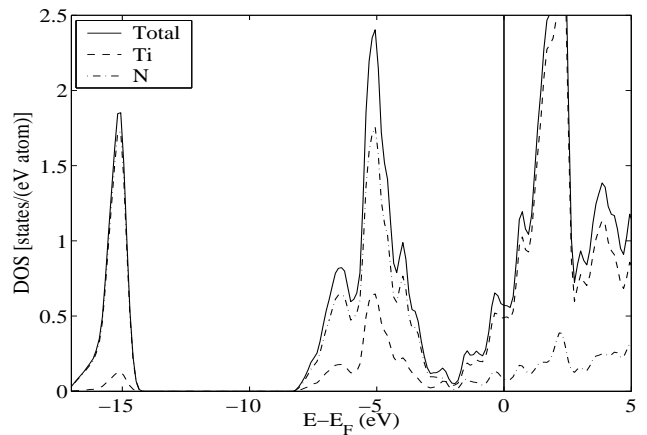


FIG. 1: Calculated total and atom-projected densities of states (DOS) for bulk TiN.

IV. RESULTS FOR TiN

A. Bulk structure, energetics, and bonding nature

Like TiC, bulk TiN adopts the rocksalt structure. Our structure optimization yields a lattice constant of 4.244 Å (experiment: 4.238 Å [10]) and a cohesive energy of 13.79 eV. Compared to TiC, the electronic structure of TiN shows strong similarities, with a DOS (Fig. 1) consisting of bonding (in the UVB) and antibonding (in the CB) Ti-N states, but also differences: (i) a higher position of E_F , shifting the CB, UVB, and LVB to lower energies; (ii) a population of antibonding states in the CB, due to the extra electron per formula unit, which lowers the cohesion energy; and (iii) a larger separation between UVB and CB, reflecting the higher ionicity of TiN (Bader charge transfer of 1.62 electrons).

B. Surface energetics and structure

The preferred termination of $TiN(111)$ has only been addressed in theoretical studies, showing that the surface is N terminated when in an N-rich environment [11]. In order to compare the stabilities of the Ti and N terminations in vacuum, we follow the approach used by Ref. [12] to show why $TiC(111)$ is Ti terminated and compare the evaporation rates for N and Ti from $TiN(111)$. While our calculated evaporation energies for $TiC(111)$ [$E_{evap} = 5.40$ (9.43) eV/atom for C (Ti)] confirm the results of Ref. [12], our values for $TiN(111)$ [$E_{evap} = 6.83$ (6.98) eV/atom for N (Ti)] imply that both Ti and N are possible terminations. Therefore, since our focus here is to find general adsorption mechanisms and to compare TiN with TiC, we study the Ti termination for both surfaces.

Our $TiX(111)$ slabs are stoichiometric. Hence, our calculations yield only values for the sum of the surface en-

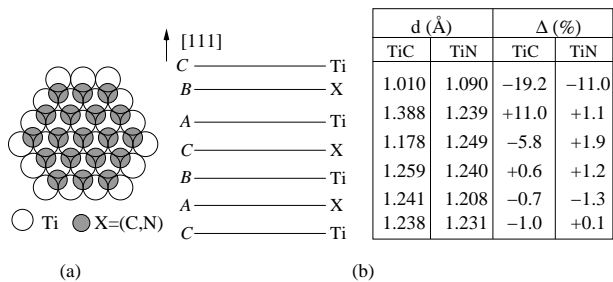


FIG. 2: Surface structure of TiX(111): (a) top view of the two surface atomic layers; (b) side view of the seven surface atomic layers, showing the ABC stacking of alternating Ti and X layers and our calculated relaxations, in absolute values (d) and relative (Δ) to the bulk interlayer distances (1.251 Å for TiC and 1.225 Å for TiN).

ergies of the Ti- and X-terminated surfaces. This corresponds to the energy cost of cleaving the infinite crystal into two semi-infinite ones. Our calculated values are: $E_{\text{cleav}} = 9.81$ (11.74) J/m² for the unrelaxed TiN (TiC) surface and $E_{\text{cleav}} = 9.17$ (11.43) J/m² after relaxation of only the Ti-terminated side of the TiN (TiC) slab. These values should be compared with those for the non-polar (001) surface, 2.76 (3.46) J/m² for TiN (TiC) [13]. Thus, for both TiX's, the polar (111) surface has a much lower stability than the (001) surface. Also, we note that surface formation is easier on TiN than on TiC.

Our relaxed surface structure of the Ti-terminated TiN(111) surface (Fig. 2) is in good agreement with the results of Ref. [10]. The relaxation is smaller than on TiC(111) and does not follow the alternating positive-negative relaxation typical of metals that is obtained for TiC(111). At the same time, it can be noted that the relaxations are larger than those typical for metals.

C. Adsorption energetics and structure

Our trend study for atomic adsorption on the Ti-terminated TiN(111) comprises the same adatoms as those considered on TiC(111), however, with larger focus on the second-period adatoms. The results for the adsorption energies E_{ads} (Fig. 3 and Table I) show many similarities to those for TiC(111): (i) at least for C, N, O, and F, a preference for the fcc site, followed by the hcp and top sites, while the bridge site relaxes to fcc; (ii) a large variety in adsorption strength, from O ($E_{\text{ads}} = 8.4$ eV in the fcc site) to Al (3.5 eV in the fcc site); (iii) overall strongest adsorption for O, C, N, S, and F; (iv) very pronounced pyramid-shaped E_{ads} trends for both adatom periods (with the exception of C), with strongest adsorption for group-VI adatoms; (v) a stronger adsorption for second-period adatoms. Also, the heights of the diffusion barriers between fcc and hcp sites can be estimated from the E_{ads} values obtained after perpendicular relaxation of the bridge adatoms (Table I). These indicate

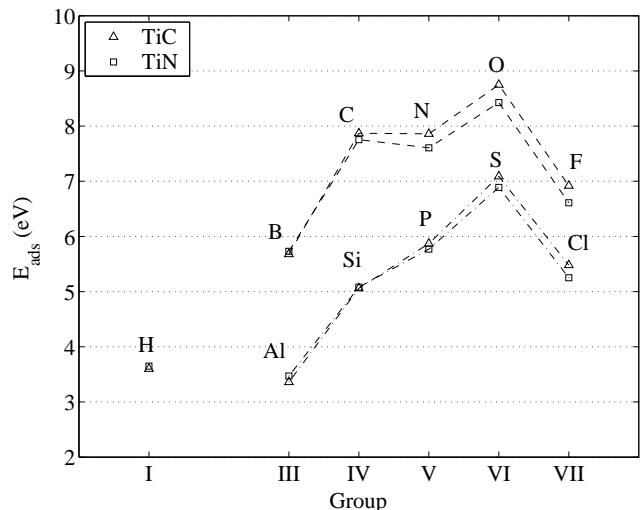


FIG. 3: Calculated atomic fcc adsorption energies E_{ads} on TiC(111) and TiN(111).

TABLE I: Calculated atomic adsorption energies E_{ads} on TiN(111) [corresponding TiC(111) values within parentheses]. For all adatoms, the bridge site is unstable and relaxes to the neighboring fcc site. The bridge values given correspond to only perpendicular relaxation.

atom	E_{ads} (eV/atom)			
	fcc site	hcp site	top site	bridge site
C	7.75 (7.87)	7.20 (7.15)	4.55 (4.69)	6.26 (6.73)
N	7.61 (7.86)	6.97 (6.87)	4.47 (4.59)	6.27 (6.77)
O	8.43 (8.75)	8.02 (7.93)	6.28 (6.50)	7.27 (7.95)
F	6.61 (6.92)	6.45 (6.46)	5.75 (6.01)	6.05 (6.58)

that the barriers are generally higher on TiN(111) than on TiC(111) (by $\sim 0.3 - 0.7$ eV for C, N, and O, and by $\sim 0.2 - 0.3$ eV for F).

It is striking how closely the E_{ads} curves for TiC(111) and TiN(111) lie, the differences being smaller than 0.32 eV. However, interesting differences arise: (i) the fcc adsorption is slightly stronger on TiN for the adatoms on the left side of each period (H, B, Al), but stronger on TiC for the adatoms on the right side (C, N, O, F, P, S, and Cl); (ii) for the fcc site, the preference for TiC adsorption increases successively when moving to the right within each adatom period; (iii) while on TiC(111), the E_{ads} values for C and N are almost the same, on TiN(111), N has a lower value than C.

The two substrates show also similarities in fcc adsorption geometries (Table II): (i) the adatom-substrate bond distances are larger for period 3 (due to the extra filled electron shell); (ii) the adatom-substrate distances are smallest for group V (in period 2) and for group VI (in period 3), and increase monotonically when moving away, in each period, from these (indicating a stronger adsorption strength for groups V–VI); (iii) the Ti–Ti distances around the adatoms decrease from the clean-surface val-

TABLE II: Calculated geometries around the fcc adatoms on TiN(111) [corresponding TiC(111) values within parentheses]: $d_{\text{ad-Ti}}$ and $d_{\text{ad-X}}$ are the distances between the adatoms and their nearest-neighbor Ti and X atoms, respectively; $Z_{\text{ad-TiX}}$ is the perpendicular distance between the adatoms and the TiX(111) surface; $d_{\text{Ti-Ti}}$ is the distance between the Ti atoms closest to the adatom (the distances in the clean surfaces are included for comparison). The Ti-X and X-X distances closest to the adatom are unaffected by the adsorption. All values are in Å.

atom	$d_{\text{ad-Ti}}$	$d_{\text{ad-X}}$	$Z_{\text{ad-TiX}}$	$d_{\text{Ti-Ti}}$
H	1.99 (2.01)	2.71 (2.73)	1.01 (1.03)	2.97 (2.98)
B	2.14 (2.16)	3.02 (3.01)	1.33 (1.32)	2.90 (2.95)
C	1.98 (1.99)	2.88 (2.86)	1.12 (1.10)	2.84 (2.88)
N	1.94 (1.94)	2.83 (2.80)	1.04 (1.02)	2.83 (2.85)
O	1.97 (1.98)	2.85 (2.81)	1.08 (1.07)	2.86 (2.88)
F	2.15 (2.16)	2.92 (2.93)	1.28 (1.28)	3.00 (3.00)
Al	2.66 (2.67)	3.56 (3.54)	2.02 (2.02)	2.99 (3.03)
Si	2.53 (2.52)	3.46 (3.39)	1.87 (1.82)	2.95 (3.00)
P	2.44 (2.44)	3.37 (3.32)	1.75 (1.72)	2.95 (2.99)
S	2.42 (2.44)	3.33 (3.30)	1.73 (1.72)	2.96 (3.00)
Cl	2.51 (2.54)	3.36 (3.35)	1.81 (1.82)	3.01 (3.06)
Clean surface	—	—	—	3.00 (3.06)

ues (indicating a strong adatom-Ti attraction), except for F and Cl, where they stay unchanged. In each period, the values for F and Cl stand out from the rest, due to their overall larger values.

V. DISCUSSION AND CONCLUSIONS

Our results for atomic chemisorption on TiC(111) and TiN(111) show strong similarities. Since the high chemical activity of TiC(111) has been connected to the presence of a SS, it is plausible to believe that, despite the electron-structure differences, the similar results for TiN(111) are caused by the presence of a similar SS on this surface. The preference for adsorption in fcc site confirms this, considering that the TiC(111) SS extends toward the fcc sites [3].

However, the differences raise intriguing questions: why is adsorption stronger on TiN on the left of the periodic table but stronger on TiC on the right? Also, why does the C adatom not follow the pyramid-shaped trend and instead adsorb more strongly than N? Obviously, factors beyond the d -band model [14], which has been so successful for transition metals, have to be introduced. Our previous results for adsorption on TiC(111) show the presence of two chemisorption mechanisms, involving both the SS and the UVB [3]. Since the UVB energy is shifted downwards in TiN, our concerted-coupling model could provide the answer to the E_{ads} differences between TiC and TiN. This is the subject of a separate conference contribution [15].

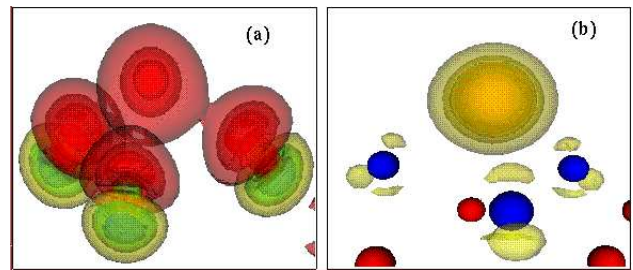


FIG. 4: Calculated differences in electron charge density for (a) O and (b) F adsorbed on TiN(111) before and after adsorption. The color coding ranges from green (electron charge depletion due to adsorption) through yellow (no charge difference) to red (electron charge increase). Blue (red) balls: Ti (N) atoms.

Also, the larger bond distances for F and Cl suggest a different bonding mechanism for these adatoms. Indeed, the differences in charge density due to adsorption (Fig. 4 shows O and F) show very weak distortions of the adatom-centered density for F, indicating a very high ionic character for this bond. In contrast, for O, the density distorts toward neighboring Ti atoms in a typical covalent fashion.

Our results might be relevant for the technological applications. The strong O adsorption indicates that TiC(111) and TiN(111) are good substrates for oxide-layer growth. Indeed, both are used in multilayer CVD alumina coatings on wear-resistant cutting tools. Our results suggest that nucleation and initial growth are similar on the two surfaces. For example, the higher adsorption energy for O than for Al suggests that the first atomic layer of the alumina coating consists of O atoms. Also, the high energy for S suggests it to be a strong competing candidate, which can explain the presence of S found in the alumina coatings under certain conditions, affecting the alumina phase composition [16]. Thus, the preference for one or another of the two substrates is more likely due to considerations related to other factors, such as mechanical properties and lattice mismatch. Also, it is likely that there are differences in electronic structure between the two O/TiX(111) systems, with implications for the continuing growth of the coating. In another context, the easy formation of a titanium-oxide layer on TiN may improve its biocompatibility [17].

Although proper bulk and growth calculations obviously are needed, our calculated diffusion-barrier estimates might be of interest for the synthesis and properties of the MAX phases. Their good plasticity is related to a weak bonding between the (111) face of the Ti_6C sheets and the A component (*e.g.*, Al or Si) [1]. Our calculated E_{ads} differences between fcc, hcp, and bridge sites for Al and Si on TiC(111), indicating diffusion barriers of the order of 0.1 – 0.3 eV (activation temperatures of $\sim 50 - 130$ K) [18], suggest good lateral mobility between the Al/Si and Ti_6C sheets. Also, our calculations indicate higher diffusion barriers on TiN(111), suggesting

a decrease in plasticity when substituting C with N.

Obviously, more studies addressing these questions are highly desirable. As a first step, we pursue in a separate publication a detailed comparison between TiC and TiN

of the adsorbate electronic structures, showing the applicability of the concerted-coupling model for adsorption on TiN(111) [15].

-
- [1] N.I. Medvedeva, D.L. Novikov, A.L. Ivanovsky, M.V. Kuznetsov, and A.J. Freeman, *Phys. Rev. B* 58 (1998) 16042.
- [2] C. Oshima, M. Aono, S. Zaima, Y. Shibata, and S. Kawai, *J. Less-Common Metals* 82 (1981) 69.
- [3] C. Ruberto and B.I. Lundqvist, *Phys. Rev. B* (submitted). Available online at <http://arxiv.org/abs/cond-mat/0511405>.
- [4] <http://www.camp.dtu.dk/campos>
- [5] R.F.W. Bader, *Chem. Rev.* 91 (1991) 893.
- [6] A. Dunand, H.D. Flack, and K. Yvon, *Phys. Rev. B* 31, (1985) 2299.
- [7] S.-H. Jhi, J. Ihm, S. G. Louie, and M.L. Cohen, *Nature* 399 (1999) 132.
- [8] K. Schwarz, *CRC Crit. Rev. Sol. St. Mater. Sci.* 13 (1987) 211.
- [9] D.M. Newns, *Phys. Rev.* 178 (1969) 1123.
- [10] M. Marlo and V. Milman, *Phys. Rev. B* 62 (2000) 2899.
- [11] D. Gall, S. Kodambaka, M.A. Wall, I. Petrov, and J.E. Greene, *J. Appl. Phys.* 93 (2003) 9086.
- [12] K.E. Tan, M.W. Finnis, A.P. Horsfield, and A.P. Sutton, *Surf. Sci.* 348 (1996) 49.
- [13] S.V. Dudiy and B.I. Lundqvist, *Phys. Rev. B* 69 (2004) 125421.
- [14] B. Hammer and J.K. Nørskov, in *Advances in Catalysis*, edited by B. C. Gates and H. Knözinger (Academic Press, San Diego and London 2000), Vol. 45, p. 71.
- [15] C. Ruberto, A. Vojvodic, and B.I. Lundqvist, *Surf. Sci.* (submitted).
- [16] M. Halvarsson, A. Larsson, and S. Rупpi, *Micron* 32 (2001) 807.
- [17] N. Huang, P. Yang, Y.X. Leng, J.Y. Chen, H. Sun, J. Wang, G.J. Wang, P.D. Ding, T.F. Xi, Y. Leng, *Biomaterials* 24 (2003) 2177.
- [18] A. Bogicevic, J. Strömquist, and B.I. Lundqvist, *Phys. Rev. Lett.* 81 (1998) 637.